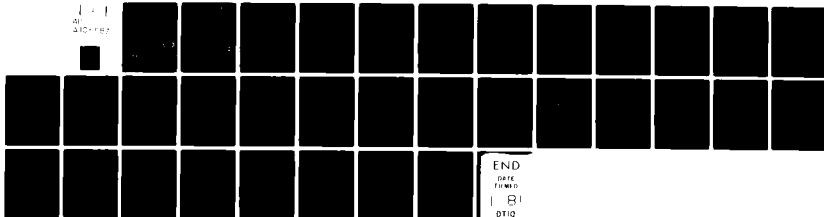


AD-A105 587

KANSAS UNIV/CENTER FOR RESEARCH INC LAWRENCE REMOTE --ETC F/G 17/9
FOUR YEARS OF LOW ALTITUDE SEA ICE BROADBAND BACKSCATTER MEASUR--ETC(U)
JUL 80 R G ONSTOTT, R K MOORE, S GOGINENI N00014-76-C-1105
CRINC/RSL-TR-331-21 NL

UNCLASSIFIED

1-1
SECRET



END
DATE
FIMED
181
DTIC

CRINC



REMOTE SENSING LABORATORY

(12) LEVEL II

AD A105587

DMC FILE COPY

DTIC
ELECTE
OCT 15 1981
S B D



THE UNIVERSITY OF KANSAS CENTER FOR RESEARCH, INC.

2291 Irving Hill Drive—Campus West
Lawrence, Kansas 66045

DISTRIBUTION STATEMENT A

Approved for public release;
Distribution Unlimited

81 8 05 020

(12) LEVEL II

(14) CR INC/RSL TR-331 2L

(6)

FOUR YEARS OF LOW ALTITUDE SEA ICE
BROADBAND BACKSCATTER MEASUREMENTS

by

R.G./ Onstott
R.K. Moore
S. Gogineni
C. Delker

(12) 34

Remote Sensing Laboratory
Center for Research, Inc.
The University of Kansas
Lawrence, Kansas 66045

RSL Technical Report
RSL TR 331-21

July 1980

Supported by:

OFFICE OF NAVAL RESEARCH
Department of the Navy
800 N. Quincy Street
Arlington, Virginia 22217

Contract No. N00014-76-C-1105

DTIC
ELECTE
OCT 15 1981
B

DISTRIBUTION STATEMENT A

Approved for public release;
Distribution Unlimited

406688

TABLE OF CONTENTS

	<u>Page</u>
LIST OF FIGURES.	ii
LIST OF TABLES	iv
ABSTRACT	1
INTRODUCTION	2
EXPERIMENT DESCRIPTION	3
SUMMARY OF RESULTS TO DATE	3
L-BAND RESULTS	6
Ku-X-BAND RESULTS.	11
EFFECT OF SNOW COVER ON THE RADAR CROSS-SECTION OF ICE	15
COMPARISON OF HELICOPTER- AND SURFACE-BASED MEASUREMENTS	19
RADAR CROSS-SECTIONS OF SEA ICE IN THE SUMMER MONTHS	25
REFERENCES	27

Accession For	
NTIS GRA&I	<input checked="" type="checkbox"/>
DTIC TAB	<input type="checkbox"/>
Unannounced	<input type="checkbox"/>
Justification	
PER LETTER	
By	
Distribution/	
Availability Codes	
Avail and/or	
Dist	Special
A	

LIST OF FIGURES

<u>Figure</u>	<u>Title</u>	<u>Page</u>
1	Average scattering coefficient of thick first-year, thin first-year, and lake ice at 1.5 GHz (March 1979)	9
2	Scattering coefficient of thick first-year, multiyear, fresh water lake, and pressure ridge ice at 1-2 GHz (May 1977).	10
3	Scattering coefficient of thick first-year and multiyear ice at 1.5, 9.0, 13.0, and 17.0 GHz (May 1977)	12
4	Scattering coefficient of thick first-year, multiyear, fresh water lake, and pressure ridge ice at 13 GHz.	13
5	Difference between radar cross-section of thick first-year and multiyear ice at 1.5, 9.0, 13.0 and 17.0 GHz with vertical polarization.	14
6	Difference between radar cross-section of thick first-year and multiyear ice at 1.5, 9.0, 13.0 and 17.0 GHz with cross-polarization	14
7	Difference between radar cross-section of thin first-year and thick first-year sea ice at 1.5, 9.0, 13.0 and 17.0 GHz with vertical polarization (TRAMAS, March 1979)	16
8	Difference between radar cross-section of thick first-year sea ice and lake ice at 1.5, 9.0, 13.0 and 17.0 GHz with vertical polarization (TRAMAS, March 1979).	16
9	The response of the scattering coefficient of thick first-year ice, site 78, as a function of snow depth at 9, 13 and 17 GHz, an incidence angle of 55°, and HH polarization (April 1978)	17
10	Average radar cross-sections for bare-ice and snow-covered thick first-year ice at 9 GHz (April 1978)	18
11	Scattering coefficient of lake ice with bare, normal, rough, and very rough snow cover conditions at 9 GHz (March 1979).	20

LIST OF FIGURES (continued)

<u>Figure</u>	<u>Title</u>	<u>Page</u>
12	Scattering coefficient of lake ice with bare, normal, rough, and very rough snow cover conditions at 17 GHz (March 1979)	21
13	Radar cross-section contrasts of multiyear, thin first-year, and lake ice with thick first-year ice at 9 GHz and like-polarization (VV) for the TRAMAS and HELOSCAT radars.	22
14	Radar cross-section contrasts of multiyear, thin first-year, and lake ice with thick first-year ice at 13 GHz and like-polarization (VV) for the TRAMAS and HELOSCAT radars.	23
15	Radar cross-section contrasts of multiyear, thin first-year, and lake ice with thick first-year ice at 17 GHz and like-polarization (VV) for the TRAMAS and HELOSCAT radars.	24
16	Scattering coefficients of thick first-year, multi-year, thin first-year, new, and pressure-ridged ice at 9 GHz and like-polarization (VV) under summer conditions (August 1980)	26

LIST OF TABLES

<u>Table</u>	<u>Title</u>	<u>Page</u>
1	TRAMAS and HELOSCAT Nominal System Specifications.	4
2	Surface-Truth Information.	5
3	Summary of Experiments to Date	7
4	Classification of Arctic Sea Ice	8

✓ P-1 7-11-11

ABSTRACT

The ability to use radar to discriminate Arctic Sea ice types has been investigated using surface-based and helicopter-borne scatterometer systems. The surface-based F-119W radar operated at 1.5 GHz and at multiple frequencies in the 8-18 GHz region. Measurements were made at angles of 10° to 70° from nadir. The helicopter-based radar operated at the 8-18 GHz frequencies with incidence angles of 0° to 60° . Extensive surface-truth measurements were made at or near the time of backscatter measurement to describe the physical and electrical properties of the polar scene. Measurements in the 8-18 GHz region verify the ability to discriminate multiyear, thick first-year, thin first-year, and pressure-ridged sea ice and lake ice. The lowest frequency, 9 GHz, was found to provide the greatest contrast between these ice categories, with significant levels of separation existing between angles from 15° to 70° . The radar cross-sections for like antenna polarizations, VV and HH, were very similar in absolute level and angular response. Cross-polarization, VH and HV provided the greatest contrast between ice types. The 1.5 GHz measurements showed that thick first-year, thin first-year, and multiyear sea ice cannot be distinguished at 10° to 60° incidence angles with like polarization, VV, by backscatter alone; but that undeformed sea ice can be discriminated from pressure-ridged ice and lake ice. The effect of snow cover on the backscatter from thick first-year ice was also investigated. It contributes on the order of 0 to 4 dB, depending on frequency and incidence angle; the contribution of the snow layer increased with increasing frequency. Snow cover on smooth lake ice was found to be a major backscatter mechanism. Summer measurements demonstrate the inability to extend the knowledge of the backscatter from sea ice under spring conditions to all seasons.

INTRODUCTION

Recent scientific and operational interests in the ice cover of the Arctic Ocean have resulted in an extensive set of experiments involving the use of radar for monitoring the properties of sea ice [1-6]. Most of the experiments by other investigators have used aircraft-borne scatterometers and imaging radars, while the University of Kansas experimenters have concentrated on surface-based and near-surface helicopter-based measurements. The aircraft measurements were usually at a single frequency and occasionally at two frequencies. The University of Kansas measurements were over a wide range of frequencies (initially, 1.5 GHz, L-band, and 8-18 GHz, Ku-X-band, and more recently, just 8-18 GHz). The purpose of all of these experiments is to gain more information about the ice and about the radar methods for measuring its properties.

The University of Kansas experiments with the surface-based system started in May of 1977 on the fast ice off Point Barrow, Alaska [7]. These investigations were followed in April of 1978 by surface and helicopter experiments at Point Barrow [8]; in March of 1979, as a part of the Canadian Surveillance Satellite program, by surface- and helicopter-based experiments off the Mackenzie Delta [9]; and in August of 1980 by experiments from a Swedish icebreaker, the YMER, in the pack ice north and west of Svalbard [10].

The basic objectives of the research are: (1) to establish the ability of radar to discriminate ice features; (2) to identify optimum frequency, polarization and incidence angle for ice discrimination; (3) to compare carefully controlled L-band measurements with those using SEASAT SAR (the experimental phase of this is essentially complete); (4) to develop a better understanding, theoretical, empirical, and experimental, of radar-ice interactions.

EXPERIMENT DESCRIPTION

Active microwave sensors integrated with a surface-based structure and small- and medium-size helicopters were used to procure backscattering cross-section per unit area (σ^0) data. These measurements using the University of Kansas TRAMAS, surface-based, and the HELOSCAT, helicopter-borne, scatterometer systems (Table 1) made use of frequency and spatial averaging to reduce signal scintillation caused by the phenomenon of fading. Absolute calibration ensues through comparison of the measured return from the polar scene and the measured return from a Luneberg lens reflector of known radar cross-section. In conjunction, surface observations were made to describe the physical and electrical properties of the ice features (Table 2).

Many types of experiments were performed in the investigation. Angular, polarization, and frequency responses were obtained with both the surface- and helicopter-based sensors. Multiple locations on an ice floe were investigated to get spatial sampling. Also, the snow layer within the radar footprint was modified to determine the effect of snow cover on the backscatter cross-section of ice. Features such as ridging, snowpack, and melt pools were also observed.

SUMMARY OF RESULTS TO DATE

Three experimental data sets have been obtained during the spring in the Beaufort Sea and one during the summer in the Greenland Sea and Arctic Ocean. Most of the experiments have been on ice that has been attached to land because of the difficulty of getting out to the pack ice during the spring season when the fast ice extends far from shore. The 1980 summer

TABLE 1: TRAMAS and HELOSCAT Nominal System Specifications

	TRAMAS 8-18	TRAMAS 1-2	HELOSCAT I	HELOSCAT II
Type	FM-CW	FM-CW	FM-CW	FM-CW
Frequency Range	8-18 GHz	1.5 GHz	8-18 GHz	8-18 GHz
Modulating Waveform	Triangular	Triangular	Triangular	Triangular
FM Sweep: ΔF	1.0 GHz	800 MHz	1.0 GHz	1.0 GHz
Transmitter Power	15 dBm	19 dBm	15 dBm	15 dBm
Intermediate Frequency	50 kHz	50 kHz	50 kHz	50 kHz
IF Bandwidth	13.5 kHz	13.5 kHz	13.5 kHz	13.5 kHz
Antennas:				
Receive Type	46 cm Reflector	91 cm Reflector	46 cm Reflector	31 cm Reflector
Transmit Type	31 cm Reflector	Standard Gain Horn	31 cm Reflector	31 cm Reflector
Feeds	Dual Ridged Horn	Log Periodic	Dual Ridged Horn	Dual Ridged Horn
Polarization Capabilities	HH, HV, VV, VH	VV, VH	VV	VV, HH
Transmit Beamwidth	8.2° at 8 GHz 4.0° at 17.7 GHz	37°	8.2° at 8 GHz 4.0° at 17.7 GHz	8.2° at 8 GHz 4.0° at 17.7 GHz
Receive Beamwidth	5.3° at 8 GHz 2.3° at 17.8 GHz	9.5°	5.3° at 8 GHz 2.3° at 17.8 GHz	8.2° at 8 GHz 4.0° at 17.8 GHz
Incidence Angles	10° - 75°	10° - 75°	20°, 40°, 60°	0°, 13°, 25°, 38°, 50°
Calibration				
Internal	Signal Injection (delay line)	Signal Injection (delay line)	Signal Injection (delay line)	Signal Injection (delay line)
External	Luneberg Lens Reflector	Luneberg Lens Reflector	Luneberg Lens Reflector	Luneberg Lens Reflector
Altitude or Target Distance	10.9 m	6.5 m	15 m	15 m

TABLE 2
SURFACE-TRUTH INFORMATION

For every site --

- 1) Classification of ice type
- 2) Air temperature
- 3) *Air-snow interface temperature*
- 4) Snow depth
- 5) Snow-ice interface temperature
- 6) Ice thickness
- 7) Description of surface condition -- both large and small scale

Additional detailed study --

- 1) Ice salinity profile
- 2) Description of vertical inhomogeneities (visual and vertical thin sections of ice cores)
- 3) Description of horizontal inhomogeneities (thin sections of ice cores)
- 4) Ice temperature profiles
- 5) Snow density
- 6) Preferred crystal orientation

expedition was the first measurement in pack ice. Table 3 summarizes the experiments performed to date. Classification of Arctic sea ice according to age or thickness is shown in Table 4.

L-BAND RESULTS

Measurements were made under spring conditions with a calibrated surface-based radar that swept from 1.1 to 1.9 GHz. These measurements were initiated to obtain a calibrated data base to determine in advance what was going to be seen by the SEASAT SAR, and then to aid in the interpretation of the SAR data. It was found from the surface-based measurements that there is no contrast between sea-ice types at these frequencies and at the SEASAT pointing angle of 20° (Figures 1 and 2). Comparison of the backscatter coefficients acquired for multiyear, thick first-year, thin first-year and lake ice, and a small pressure-ridge with the results obtained from imaging radars [11,12, 13] indicates that the utility of an L-band radar is in distinguishing between prominent features such as linear ridges, relatively flat areas of pack ice, land, and lake ice. The angular response of the backscattering cross-section does suggest, however, that if angles greater than 50° and like polarization (VV) are used, multiyear ice may be discriminable from thick and thin first-year ice.

Multiyear, pressure-ridged, and lake ice showed less sample-to-sample variability than would be expected on the basis of surface scattering, indicating that volume scattering plays a role in their scattering processes. This may prove useful in interpreting imagery using an L-band radar. As an example, because of the additional samples in each measurement, multiyear ice floes will have textural tones which are more uniform than floes of thick first-year ice.

TABLE 3 -- Summary of Experiments to Date

ICE TYPE	MARCH	APRIL	MAY	JUNE	JULY	AUGUST	SEPTEMBER	OCTOBER	NOVEMBER
Multiyear			TRAMAS (77)			HELOSCAT II (80)			
Thick First-Year	TRAMAS (79) HELOSCAT I (79)	TRAMAS (78) HELOSCAT I (78)	TRAMAS (77)			HELOSCAT II (80)			
Thin First-Year	TRAMAS (79) HELOSCAT II (79)					HELOSCAT II (80)			
Young						HELOSCAT II (80)			
New						HELOSCAT II (80)			
Brackish	HELOSCAT I (79)								
Pressure-Ridged			TRAMAS (77)			HELOSCAT II (80)			
Lake	TRAMAS (79) HELOSCAT I (79)	HELOSCAT I (78)	TRAMAS (77)						

Pol: VV, VH, VV, VH, HH, HV
 Pol: VV
 Pol: VV, HH

Angles: 0° to 70°
 Angles: 20°, 40°, 60°
 Angles: 20°, 40°, 60°
 Angles: 0°, 13°, 25°, 38°, 50°

TRAMAS Freq: 1.5, 9, 10, 11, 12, 13, 14, 15, 16, 17 GHz
 HELOSCAT I (78) Freq: 1.5, 9, 10, 11, 12, 13, 14, 15, 16, 17 GHz
 HELOSCAT I (79) Freq: 9, 10, 11, 12, 13, 14, 15, 16, 17 GHz
 HELOSCAT II (80) Freq: 9, 10, 11, 12, 13, 14, 15, 16, 17 GHz

TABLE 4
CLASSIFICATION OF ARCTIC SEA ICE

1) Open water	
2) New ice	0-5 cm
3) Thin young ice	5-18 cm
4) Thick young ice	18-30 cm
5) Thin first-year ice	30-90 cm
6) Thick first-year ice	90-180 cm
7) Multiyear ice	180-360 cm

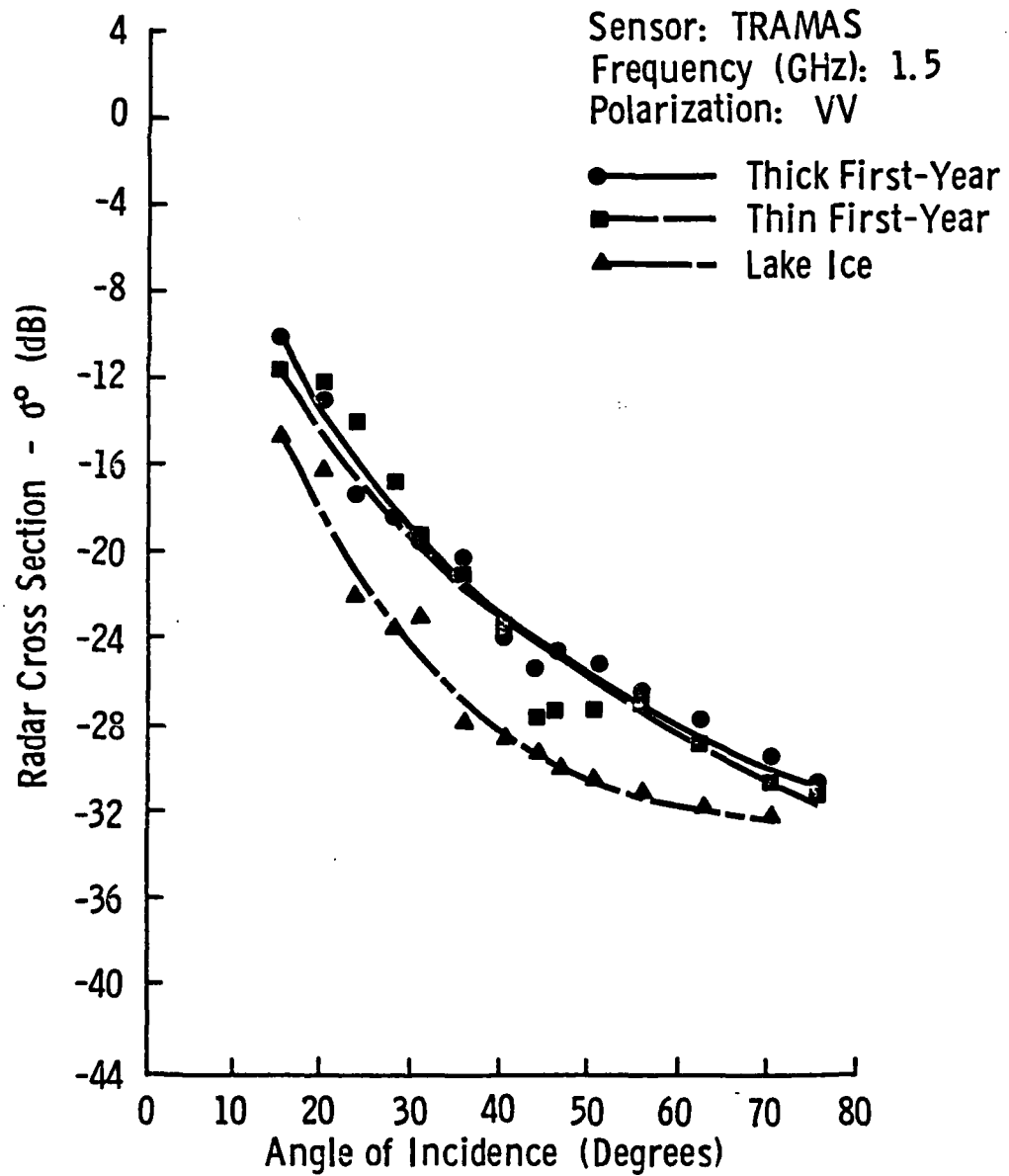


Figure 1. Average Scattering Coefficient of Thick First-Year, Thin First-Year, and Lake Ice at 1.5 GHz (March 1979)

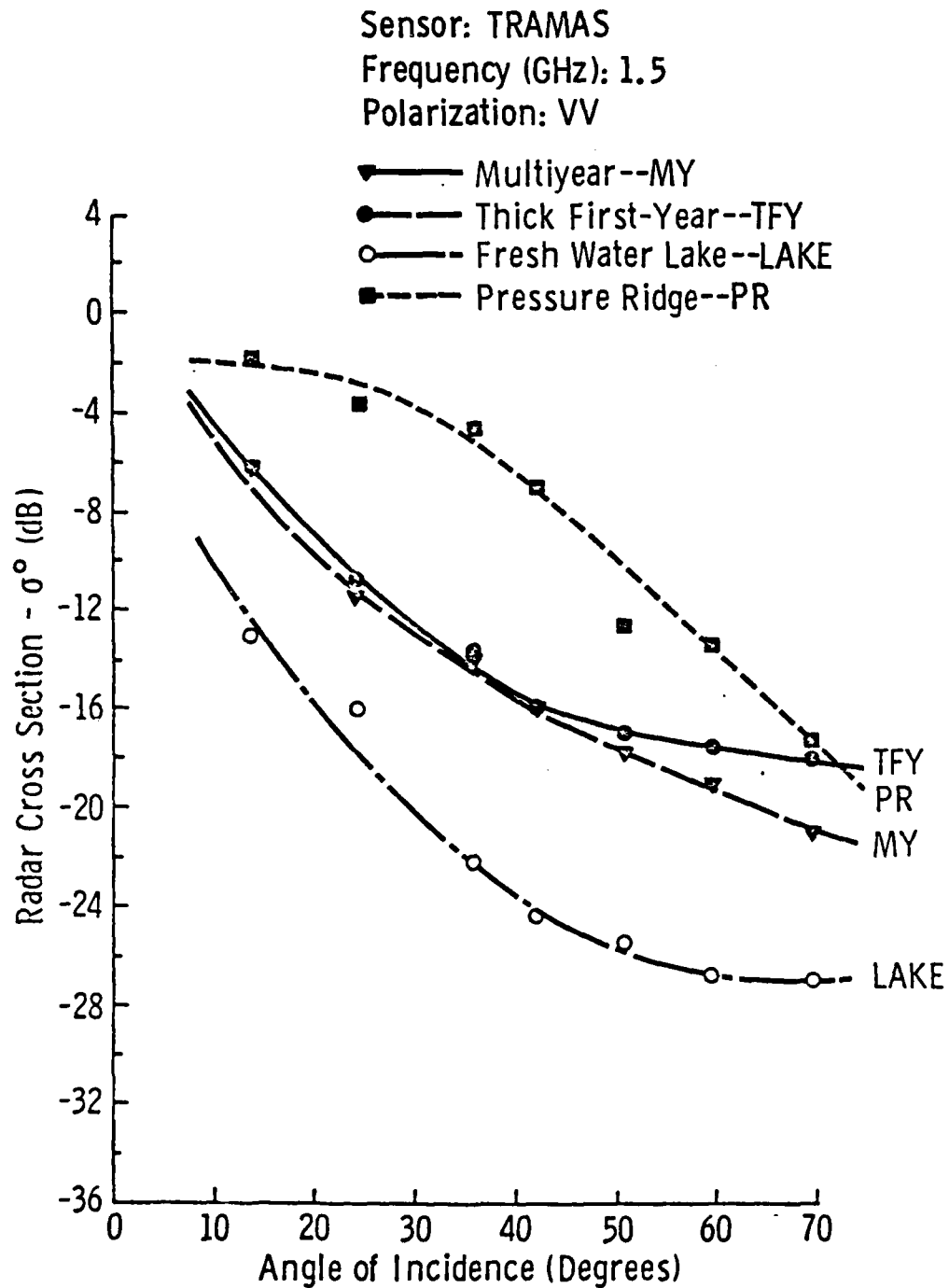


Figure 2. Scattering Coefficient of Thick First-Year, Multiyear, Fresh Water Lake, and Pressure Ridge Ice at 1.5 GHz (May 1977).

Ku-X-BAND RESULTS

A general conclusion that may be drawn from the measurements acquired during the springs of 1977, 1978, and 1979 is that 9 GHz is the best of the frequencies used for most discrimination between ice types. The middle angles of incidence (30° to 60°) appear most suitable for ice-type discrimination. The 1980 summer data are still being analyzed, and general conclusions have not been made.

Strong similarities exist between the angular responses of the radar cross-sections at different frequencies in the 8-18 GHz frequency range (Figure 3). The response of multiyear ice, a small pressure-ridge, thick first-year ice, and lake ice shown in Figure 4 is typical of like-polarization. Vertical and horizontal polarizations were nearly identical in response for small angles of incidence, but at larger angles vertical polarization is slightly higher in absolute level. A possible reason for higher vertical polarization return is the presence of small-scale surface roughness [14,15]. Physically, the vertically-polarized wave is more sensitive to surface slopes than the horizontally-polarized wave when the surface roughness is small compared to the incident wavelength. Cross-polarization resulted in much lower but still measurable radar cross-sections. This suggests that back-scatter from these ice types is not purely surface scatter. A purely surface-scattering relatively smooth medium returns extremely low cross-polarization signal levels which probably are below the noise level of the instrument.

The difference between the radar cross-sections of multiyear and thick first-year ice is shown in Figures 5 and 6 for angles from 10° to 70° and like- and cross-polarization. These results, obtained with the surface-based

Sensor: TRAMAS

Polarization: VV

Multiyear--MY

Thick First-Year--TFY

Polarization: VV

Frequency (GHz):

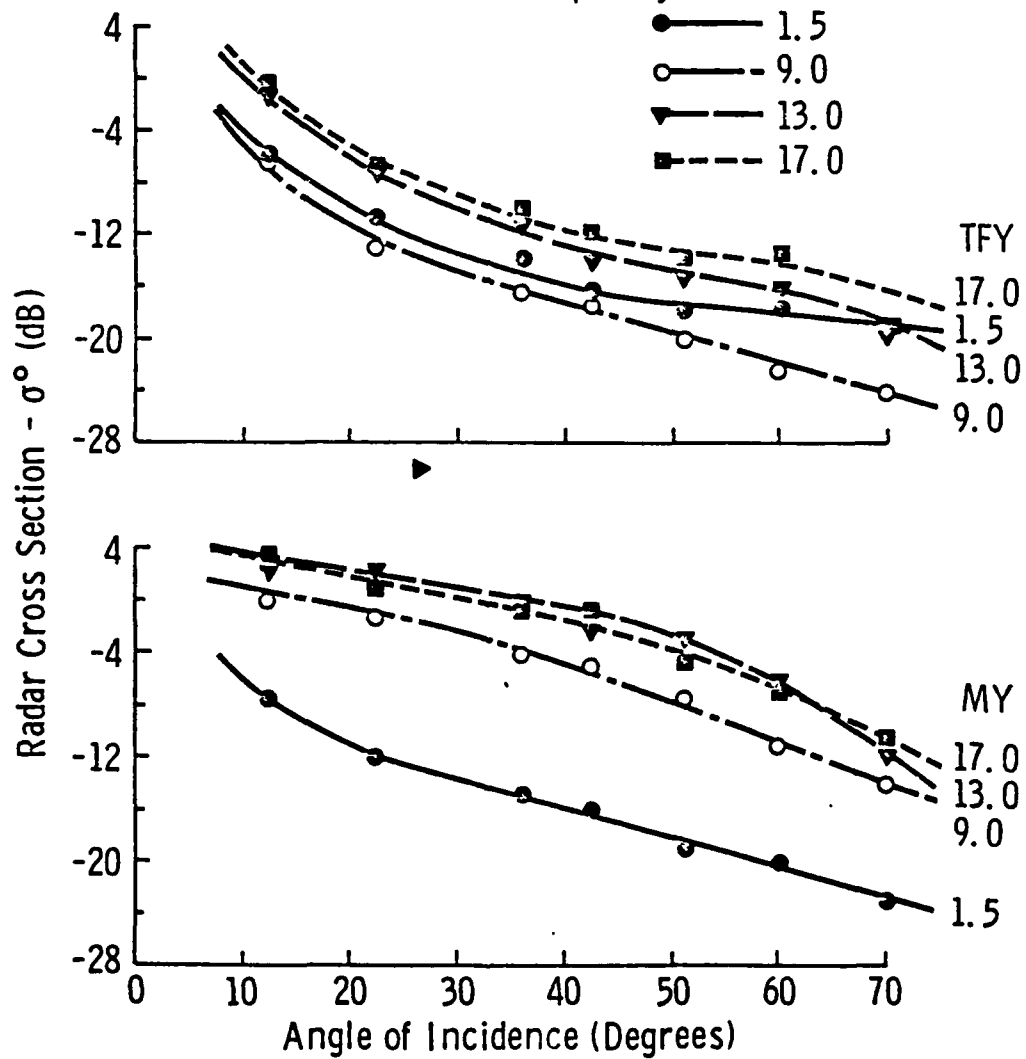


Figure 3. Scattering Coefficient of Thick First-Year and Multiyear Ice at 1.5, 9.0, 13.0, and 17.0 GHz (May 1977).

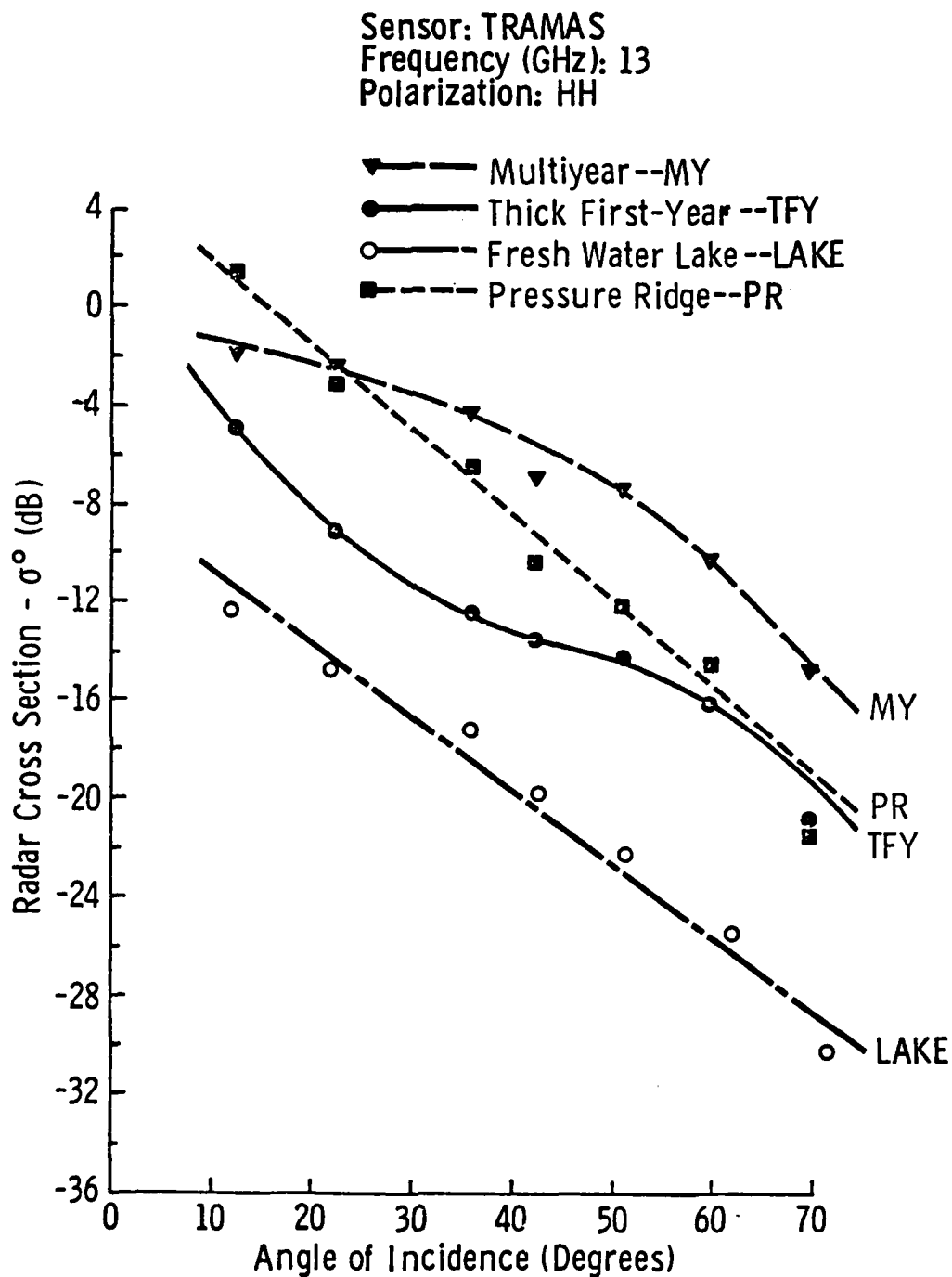


Figure 4. Scattering Coefficient of Thick First-Year, Multiyear, Fresh Water Lake, and Pressure Ridge Ice at 13 GHz (May 1977).

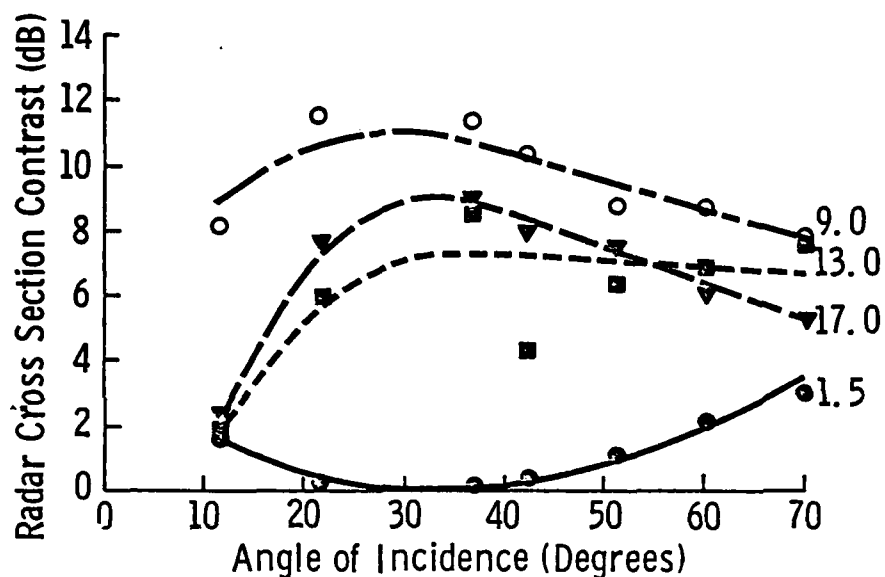


Figure 5. Difference Between Radar Cross Section of Thick First-Year and Multiyear Ice at 1.5, 9.0, 13.0, and 17.0 GHz with Vertical Polarization

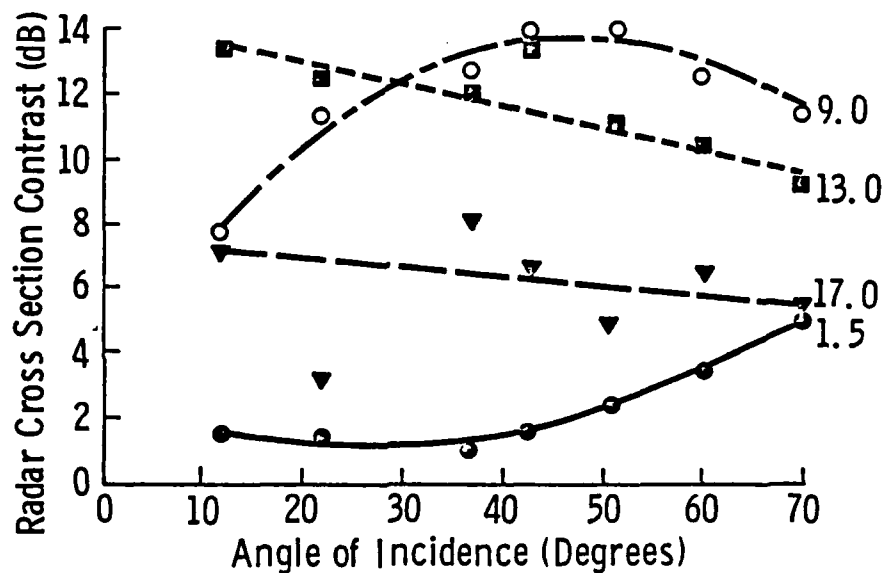


Figure 6. Difference Between Radar Cross Section of Thick First-Year and Multiyear Ice at 1.5, 9.0, 13.0, and 17.0 GHz with Cross Polarization (May 1977).

radar, indicate that 9 GHz is the better discriminating frequency. Cross-polarization and the choice of a middle incidence angle also improves contrast. Contrasts of thin first-year ice with a surface layer of salt flowers and lake ice with thick first-year ice are shown in Figures 7 and 8, respectively. Thin first-year cross-sections were higher than those of thick first-year ice, with the large angles providing the greatest contrast. The contrast between snow-covered lake ice and thick first-year sea ice acquired under very cold conditions (air = -35°C) in 1979 shows that lake-ice cross-sections were more than 5 dB lower at 9 and 13 GHz and 2 dB lower at 17 GHz than cross-sections for thick first-year ice. Contrast between lake ice with a bare surface and thick first-year ice under warm conditions (air = 0°C) in 1977 shows that lake-ice cross-sections were more than 5 dB lower. Low cross-sections from lake-ice are expected and are explained by the typically smooth air- or snow-ice interface, the low dielectric constant of snow and ice, and the sparse population of scattering sources in the ice.

EFFECT OF SNOW COVER ON THE RADAR CROSS-SECTION OF ICE

The effect of a snow layer on the radar scattering cross-section of sea and lake ice was investigated. As the thickness of the snow layer on thick first-year sea ice increased, the absolute level of the radar cross-section at the Ku-X-band frequencies also increased (Figure 9). Thus, the addition of a snow layer enhances the level of return, with differences ranging from 1-4 dB between snow-covered and bare-surfaced ice (Figure 10). The effect of a snow layer on lake ice was much more striking. Measurements were acquired under cold conditions of ice with a normal 4-cm snow-layer, a roughened snow-surface (snowmobile tracks), a gridded snow-layer (grooves

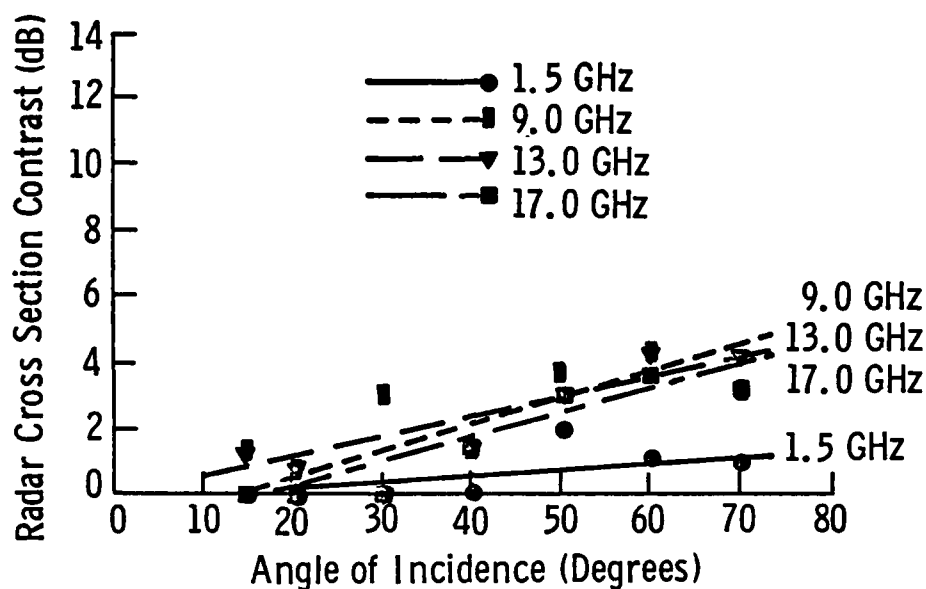


Figure 7. Difference Between Radar Cross-Section of Thin First-Year and Thick First-Year Sea Ice at 1.5, 9.0, 13.0, and 17.0 GHz with Vertical Polarization (TRAMAS, March 1979).

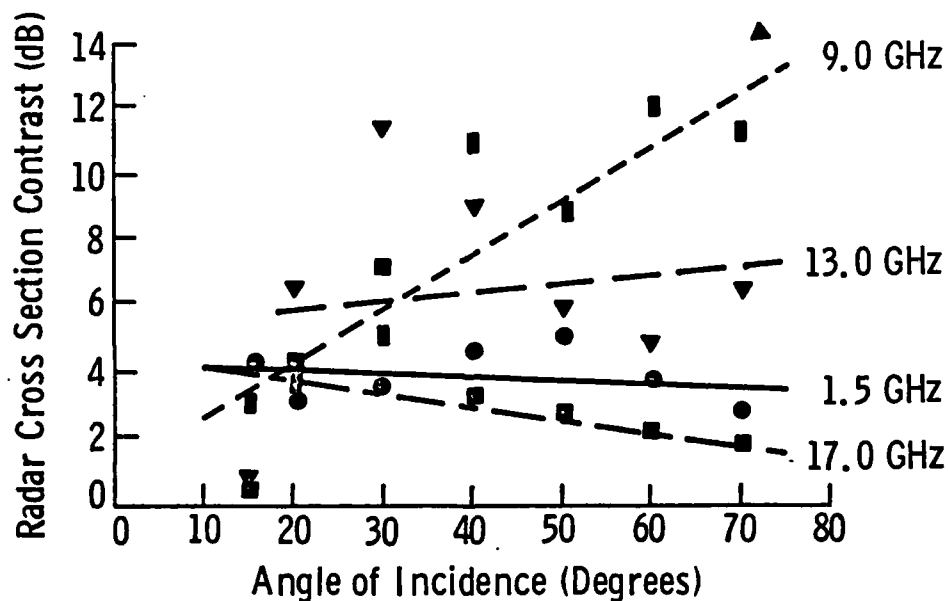


Figure 8. Difference Between Radar Cross-Section of Thick First-Year Sea Ice and Lake Ice at 1.5, 9.0, 13.0, and 17.0 GHz with Vertical Polarization (TRAMAS, March 1979).

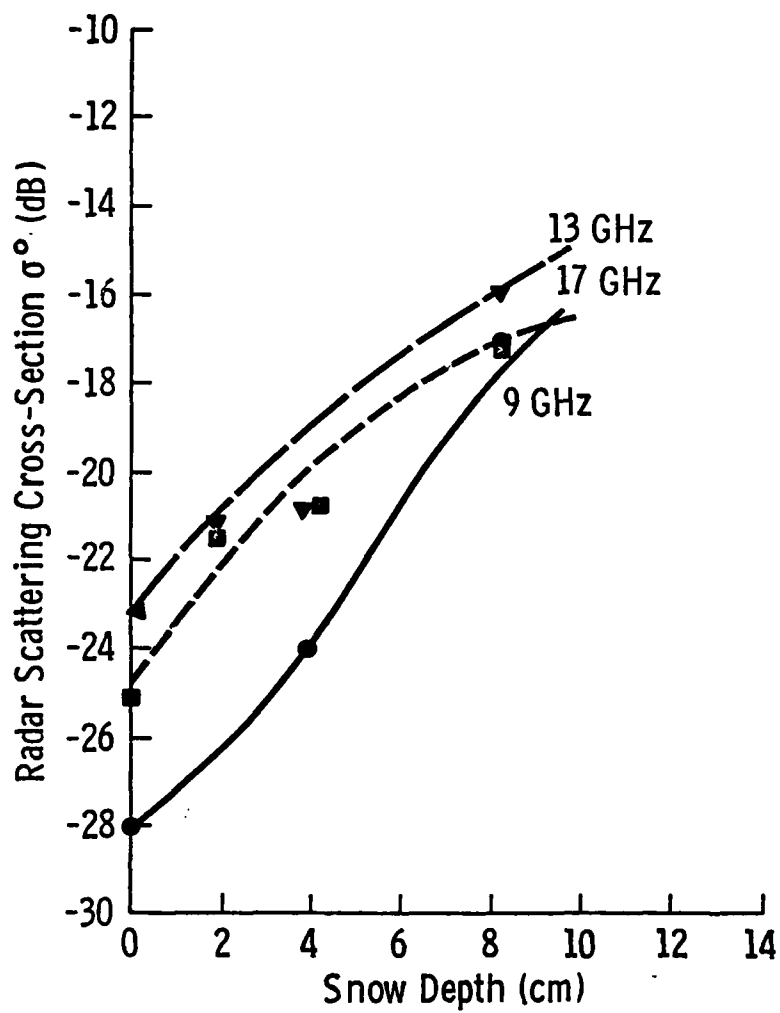


Figure 9. The Response of the Scattering Coefficient of Thick First-Year Ice, Site 78, as a Function of Snow Depth at 9, 13, and 17 GHz, an Incidence Angle of 55° , and HH Polarization (April 1978).

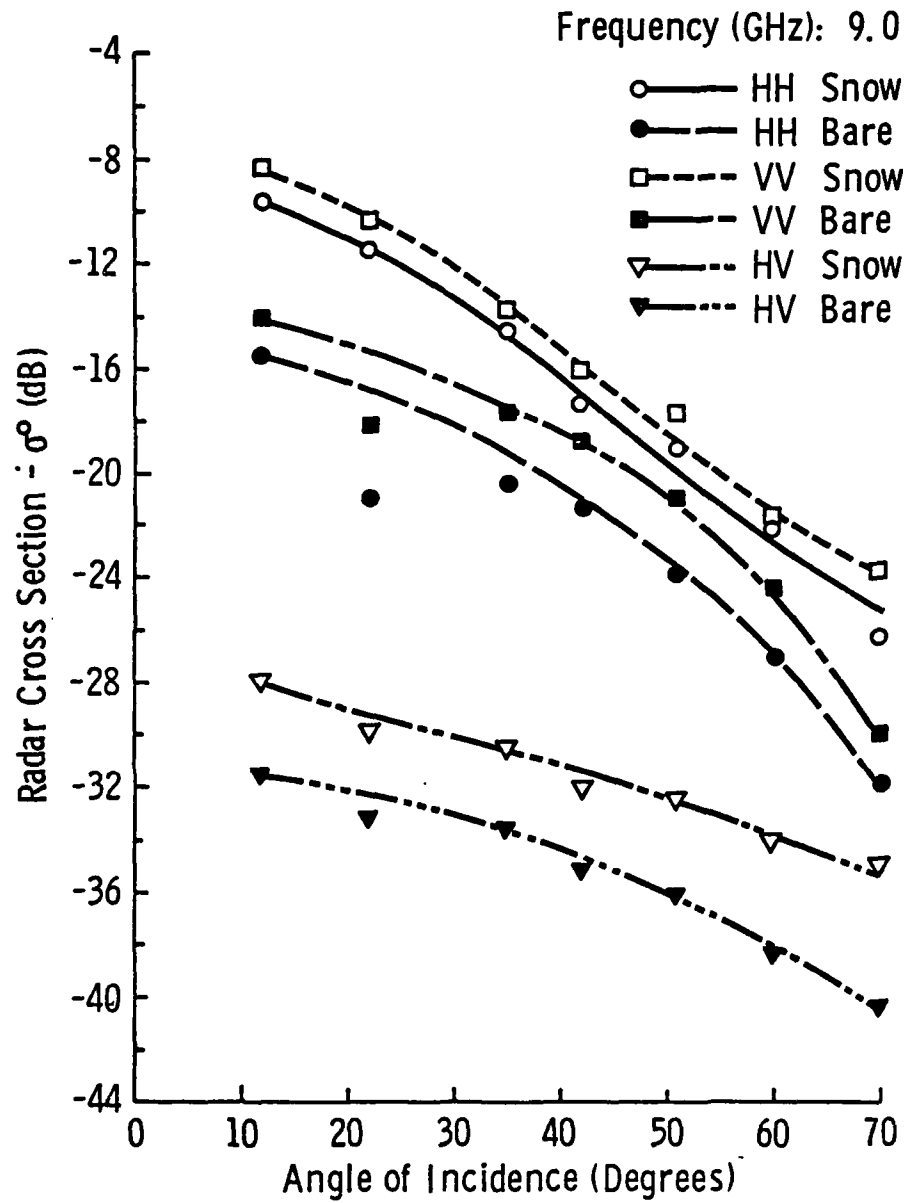


Figure 10. Average Radar Cross-Sections for Bare and Snow-Covered Thick First-Year Ice at 9 GHz (April 1978).

4-cm deep, 3-cm wide, and 15-cm spacings), and ice with the snow layer removed (Figures 11 and 12). Normal snow and roughened snow-covered ice showed similar cross-sections, with the gridded snow-covered ice having the greatest backscatter. Very large absolute-level differences (8 dB) were found to exist between ice with a bare surface and ice with a snow layer. Hence, the snow layer on sea or lake ice cannot be considered to be transparent and snow surface roughness may have a minor effect on the level of backscatter. As for lake ice, the snow layer is a major contributor to backscatter. Clearly, more exhaustive study into the effects of snow on the backscatter from ice must be performed.

COMPARISON OF HELICOPTER- AND SURFACE-BASED MEASUREMENTS

The helicopter-borne scatterometer has acquired radar cross-sections that are, in general, very similar to those described by the surface-based instrument. The cross-sections of thin first-year and lake ice are contrasted with thick first-year ice in Figures 13, 14, and 15. Examination of the level of contrast and the general angular-response of the TRAMAS and HELOSCAT radars for thin first-year and thick first-year ice shows that at 9 GHz the HELOSCAT acquired approximately a 2 dB higher contrast than the TRAMAS, at 13 GHz there is an absolute-level disagreement at 40° with the HELOSCAT seeing a 3 dB higher contrast, and at 17 GHz there is complete agreement. Contrast between lake and thick first-year ice shows that at 9 and 13 GHz the TRAMAS produced results with much greater contrast (measured a much lower scattering cross-section for lake ice) at 60°. This may be attributed to a greater signal-to-coherent-noise ratio for the surface-based instrument. In summary, the surface-based and low-altitude helicopter-borne

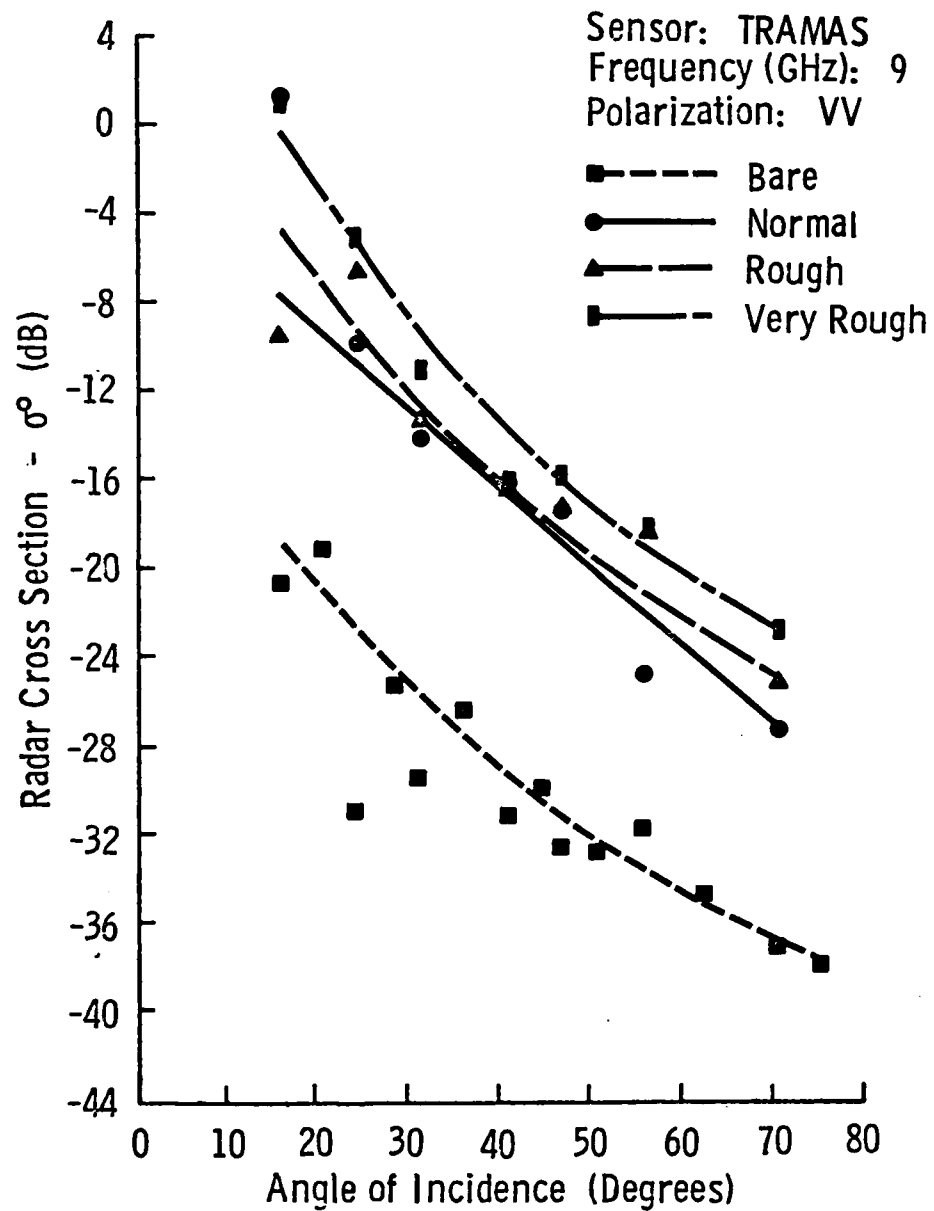


Figure 11. Scattering Coefficient of Lake Ice with Bare, Normal, Rough, and Very Rough Snow Cover Conditions at 9 GHz (March 1979).

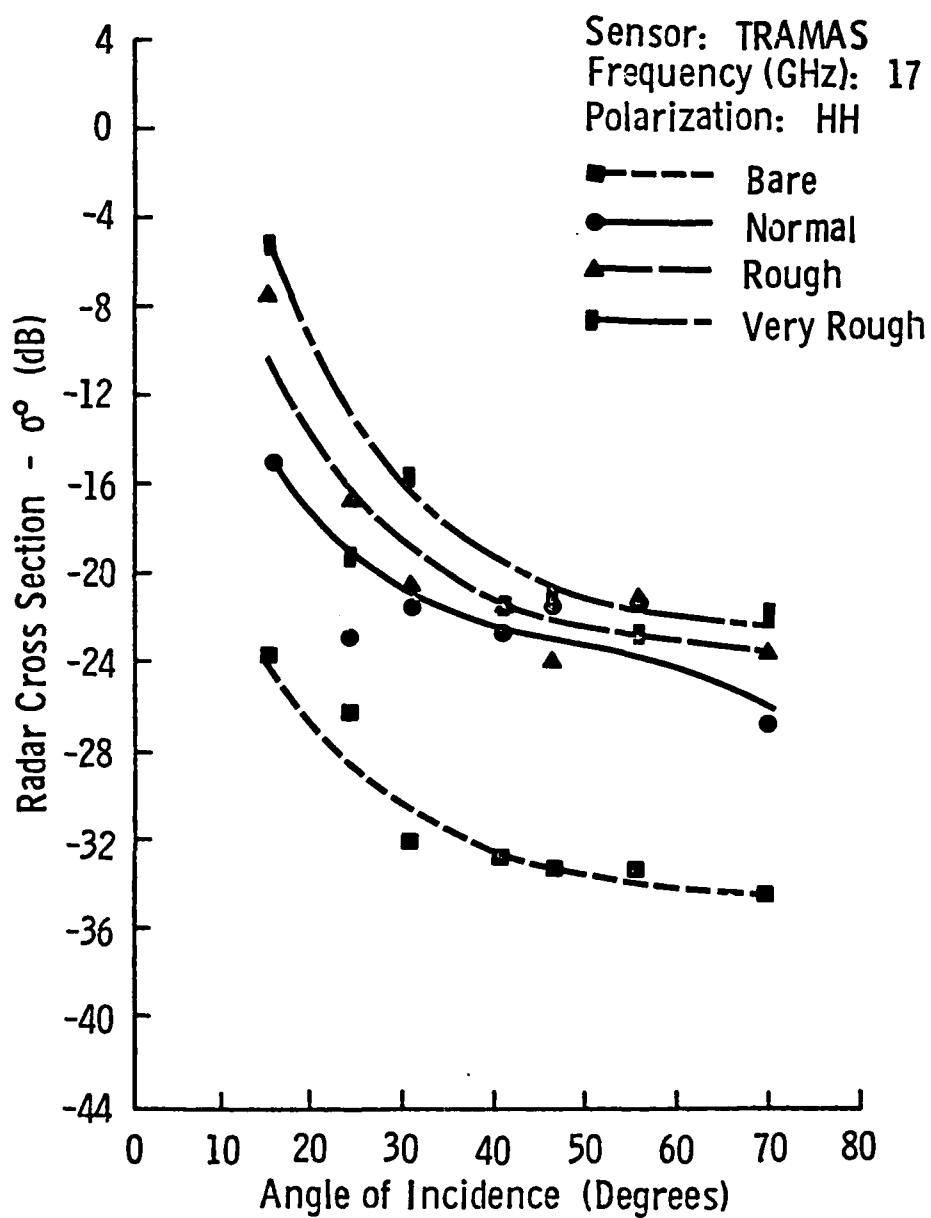


Figure 12. Scattering Coefficient of Lake Ice with Bare, Normal, Rough, and Very Rough Snow Cover Conditions at 17 GHz (March 1979).

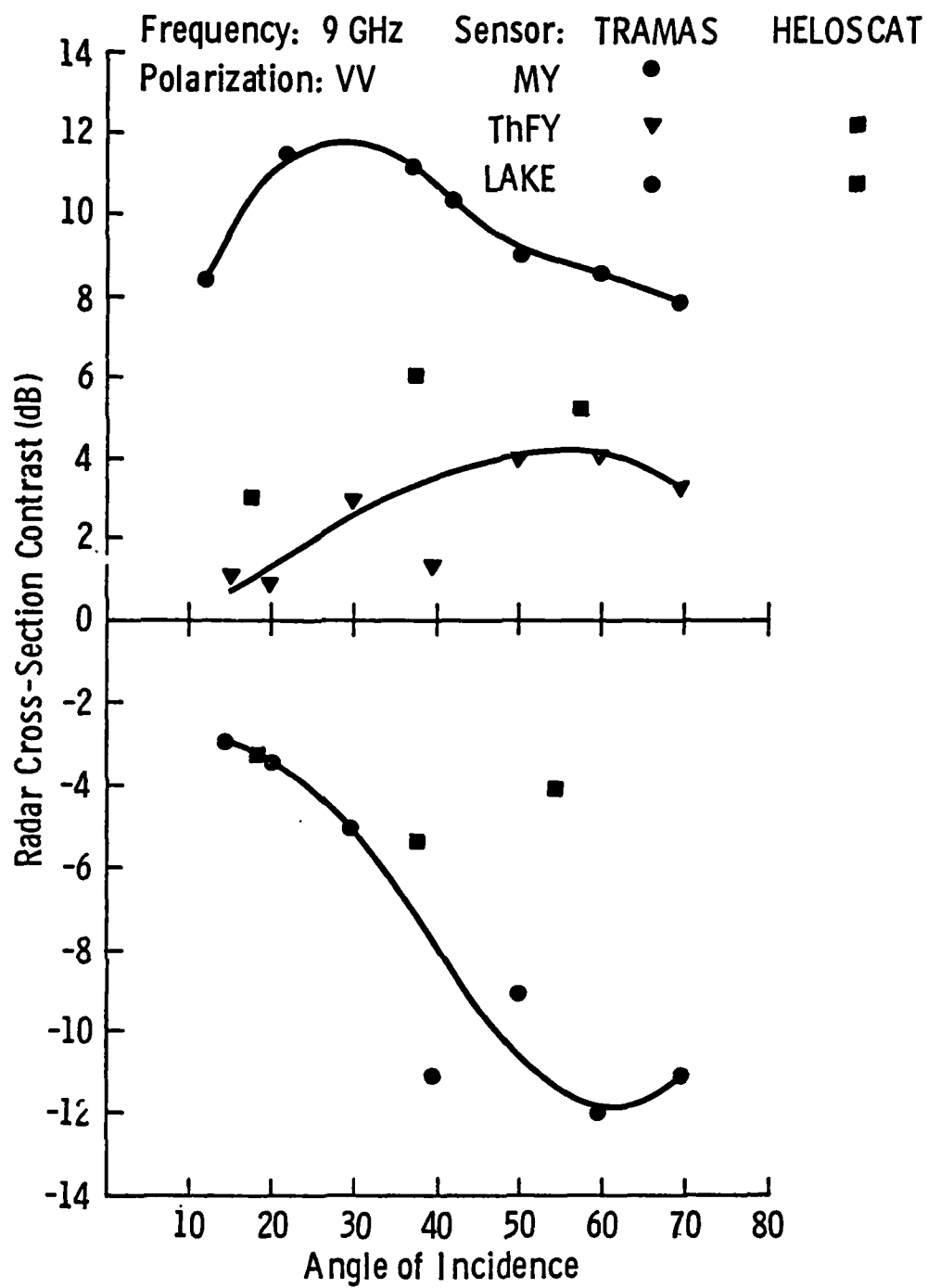


Figure 13. Radar Cross-Section Contrasts of Multiyear, Thin First-Year, and Lake Ice with Thick First-Year Ice at 9 GHz and Like-Polarization (VV) for the TRAMAS and HELOSCAT Radars.

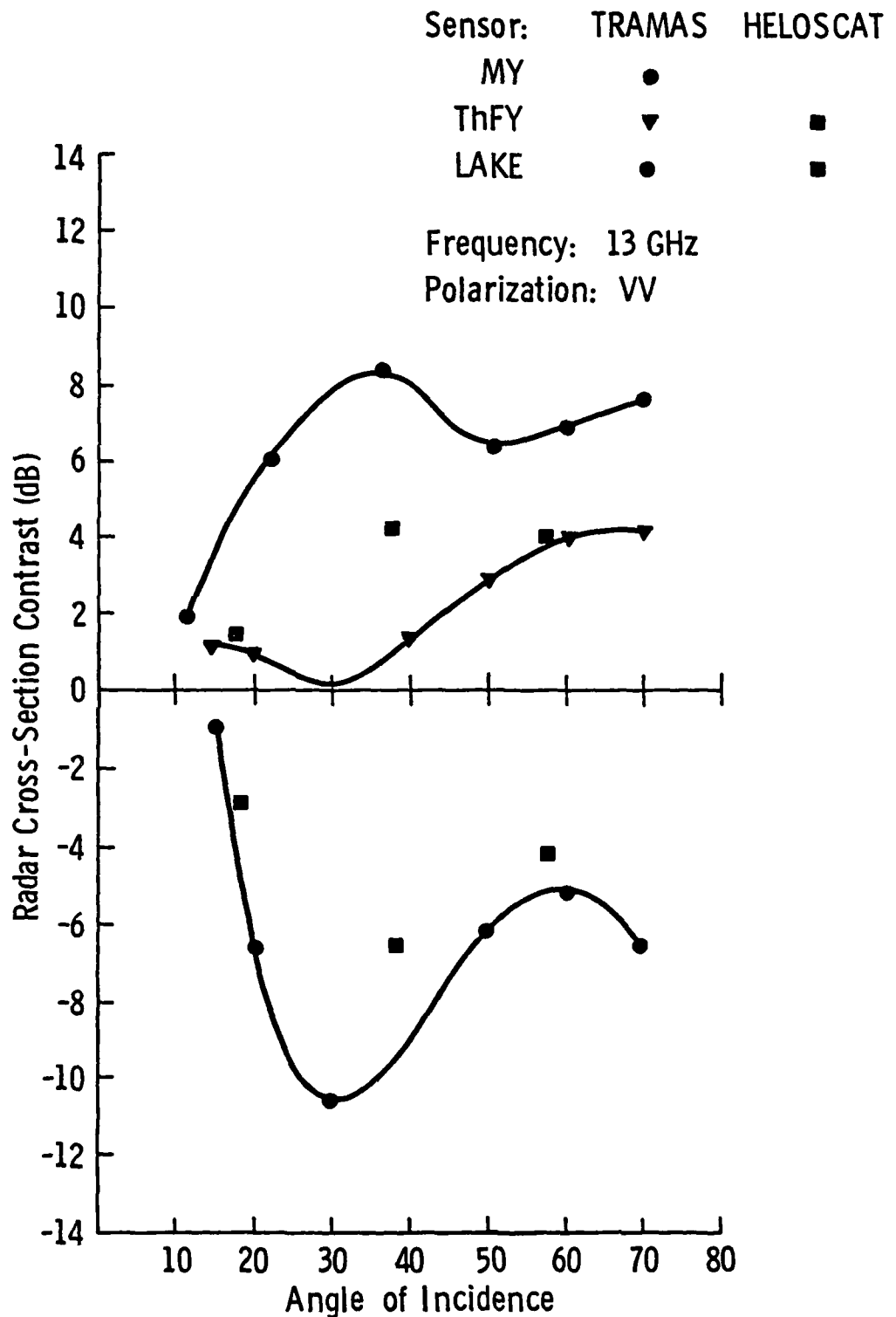


Figure 14. Radar Cross-Section Contrasts of Multiyear, Thin First-Year, and Lake Ice with Thick First-Year Ice at 13 GHz and Like-Polarization (VV) for the TRAMAS and HELOSCAT Radars.

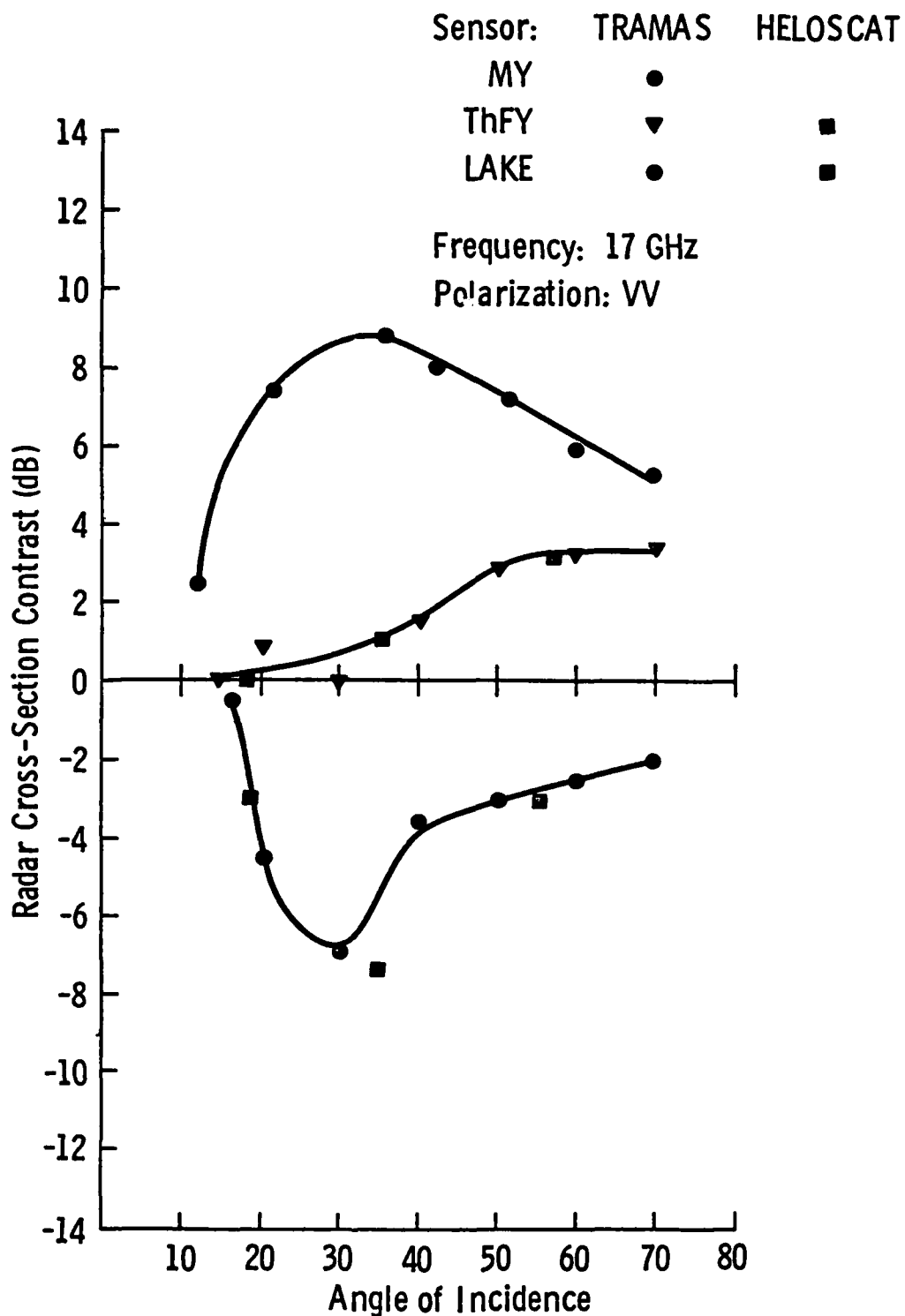


Figure 15. Radar Cross-Section Contrasts of Multiyear, Thin First-Year and Lake Ice with Thick First-Year Ice at 17GHz and Like-Polarization (VV) for the TRAMAS and HELOSCAT Radars.

radars see similar ice features with radar cross-sections contrasts that correlate well.

RADAR CROSS-SECTIONS OF SEA ICE IN THE SUMMER MONTHS

Data were acquired from pressure-ridged, thick first-year, thin first-year, multiyear, and new ice during the 1980 summer season. Preliminary results (Figure 16) demonstrate the inability to extend the knowledge of the radar backscatter from sea ice under spring conditions to all seasons. What is important to notice is the reversal of brightness trends that has occurred between thick first-year and multiyear ice. When a comparison is made between the cross-sections of spring and summer ice it is found that the multiyear ice response has changed only modestly. This correlates well with the lack of any perceivable major changes in the physical properties of the ice. However, the snowpack had gone through metamorphosis and become a solid layer of recrystallized low-salinity ice. Multiyear floes are composed of two major ice features: snowpack-and-ice and meltpools-and-ice. The number of pools was not significantly greater in the summer than in the spring. The dielectric properties and the scattering centers in the upper layers of the ice and the small-scale surface roughness remain similar between spring and summer, the number of meltpools remains on the same order, and the electrical characteristics of the snow-pack at these radar frequencies are only moderately modified, even though the snow layer has gone through a radical change in physical form. Hence, cross-sections of ice measured at nearly the same temperature in 1977 should be similar. Returns from thick first-year ice were, however, on the order of 10 dB brighter in the summer. Variations in the spatial physical properties of the ice were just as dramatic. The ice was heavily spotted with meltpools. In contrast, in the spring only snowpack-

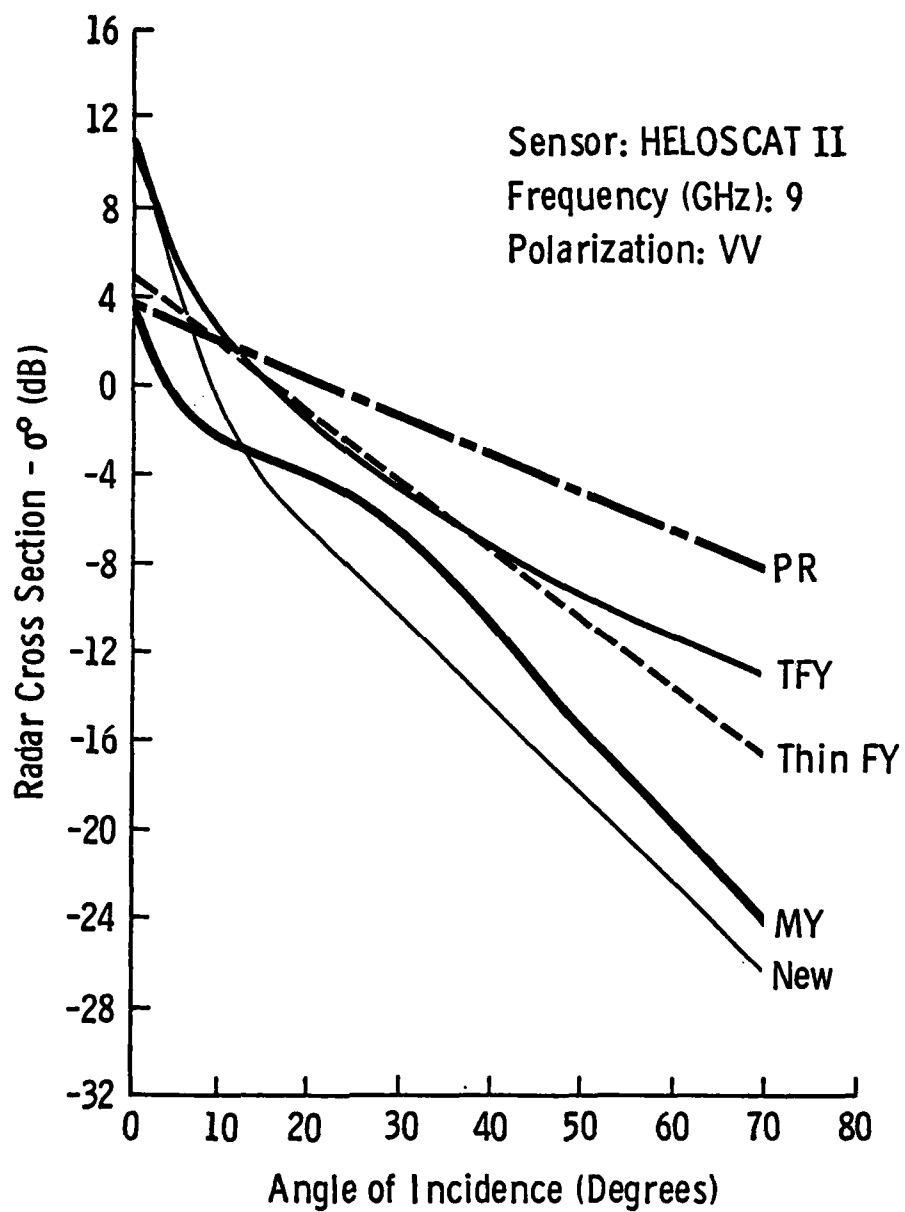


Figure 16. Scattering Coefficients of Thick First-Year, Multiyear, Thin First-Year, New, and Pressure-Ridged Ice at 9 GHz and Like-Polarization (VV) Under Summer Conditions (August 1980).

and ice conditions exist. Many of the summer melt pools were highly saline and, in some instances, melted to the sea water below. In contrast, the pools on multiyear ice were much more shallow and contained fresh water.

Noting the preliminary nature of these results, even in the summer season there appears to be an ability to discriminate among ice types (Figure 16). However, because of the dramatic change in brightness of thick first-year ice between spring and summer, a transitory period of confusion is expected to occur.

REFERENCES

- [1] Rouse, J.W. (Jr.), "Arctic Ice Type Identification by Radar," Proc. IEEE, vol. 57, 1969, pp. 605-614.
- [2] Johnson, J.D. and L.D. Farmer, "Use of Side-Looking Airborne Radar for Sea Ice Identification," J. Geophys. Res., vol 76, no. 9, 1971, pp. 2138-2155.
- [3] Parashar, S.K., A.W. Biggs, A.K. Fung, and R.K. Moore, "Investigation of Radar Discrimination of Sea Ice," Proceedings of Ninth International Symposium on Remote Sensing of Environment, Univ. of Michigan, Ann Arbor, 1974.
- [4] Gray, L., R.O. Ramseier, and W.J. Campbell, "Scatterometer and SLAR Results Obtained over Arctic Sea Ice and Their Relevance to the Problems of Arctic Ice Reconnaissance," Fourth Canadian Symposium on Remote Sensing, Quebec, Canada, May 1977, pp. 424-443.
- [5] Campbell, W.J. et al., "Microwave Remote Sensing of Sea Ice in the Aidjex Main Experiment," Boundary-Layer Meteorology, no. 3., 1978, pp. 309-337.
- [6] Livingstone, C.E. et al., "The Microwave Signatures of Sea-Ice Types and Features and Their Implications for Remote Sensing," Canada Centre for Remote Sensing, Report 1980 (in press).
- [7] Onstott, R.G., R.K. Moore and W.F. Weeks, "Surface-Based Scatterometer Results of Arctic Sea Ice," IEEE Trans. on Geoscience Electronics, vol. GE-17, no. 3, July 1979, pp. 78-85.
- [8] Onstott, R.G. et al., "Radar Backscatter Study of Sea Ice," Remote Sensing Laboratory Technical Report TR331-14, University of Kansas Center for Research, Inc., Lawrence, Kansas, February 1980.

- [9] Delker, C.V., R.G. Onstott and R.K. Moore, "Radar Scatterometer Measurements of Sea Ice: The SURSAT Experiment," Proceedings of the Final SURSAT Ice Workshop, Atmospheric Environment Service, Toronto, Canada, June 1980.
- [10] Onstott, R.G., S. Gogineni, C.V. Delker and R.K. Moore, "Measurements of Radar Backscatter from Arctic Sea Ice in the Summer," Remote Sensing Laboratory Technical Report, RSL TR331-20, University of Kansas Center for Research, Inc., Lawrence, Kansas, April 1981.
- [11] Ketchum, R.D. and S.G. Tooma, "Analysis and Interpretation of Airborne Multifrequency Side-Looking Radar Sea Ice Imagery," J. Geophys. Res., vol. 78, no. 3, 1973, pp. 520-538.
- [12] Ketchum, R.D. and L.D. Farmer, "Eastern Arctic SURSAT SAR Ice Experiment: Radar Signatures of Sea Ice Features," NORDA Technical Note 68, Naval Ocean Research and Development Activity, NSTL Station, Mississippi, August 1980.
- [13] Larson, R.W., J.D. Lyden, R.A. Shuchman and R.T. Lowry, "Determination of Backscatter Characteristics of Sea Ice Using Synthetic Aperture Radar Data," Environmental Research Institute of Michigan, Report No. 142600-1-F, Ann Arbor, Michigan, March 1981.
- [14] Wright, J.W., "A New Model for Sea Clutter," IEEE Transactions on Antennas and Propagation, vol. AP-16, no. 2, March 1978, pp. 217-223.
- [15] Moore, R.K. and A.K. Fung, "Radar Determination of Winds at Sea," Proc. IEEE, vol. 67, no. 11, November 1979, pp. 1504-1521.

DATE
ILME